THE ASTROPHYSICAL JOURNAL, 454:L31–L34, 1995 November 20

DETECTION OF ULTRAVIOLET EMISSION LINES IN SN 1006 WITH THE HOPKINS ULTRAVIOLET TELESCOPE

JOHN C. RAYMOND[1]
Harvard-Smithsonian Center for Astrophysics, 60 Garden Street, Cambridge, MA 02138; raymond@cfa.harvard.edu

WILLIAM P. BLAIR
Department of Physics and Astronomy, Johns Hopkins University, Charles and 34th Streets, Baltimore, MD 21218; wpb@pha.jhu.edu

AND

KNOX S. LONG
Space Telescope Science Institute, Baltimore, MD 21218; long@stsci.edu
Received 1995 July 24; accepted 1995 September 11

ABSTRACT

The Hopkins Ultraviolet Telescope (HUT) was used during the Astro-2 space shuttle mission in 1995 March to observe emission lines of H I, He II, C IV, N V, and O VI from the faint optical Balmer line filament at the northwest edge of the SN 1006 supernova remnant. This is the first successful far-ultraviolet observation of a nonradiative shock wave with velocity in excess of 300 km s^{-1} and the first detection of ultraviolet emission lines from SN 1006. The observed line widths are consistent with the ~2300 km s^{-1} width reported for Hα, implying that the velocities of different ions are independently randomized in the shock and that ion-ion temperature equilibration is ineffective. A faint continuum in the spectrum is consistent with relatively strong dust-scattered starlight along this line of sight, visible because of the large HUT spectrograph aperture used for this observation. The relative line intensities are in reasonable agreement with existing model predictions for a 2300 km s^{-1} shock. However, proton excitation rates may compete with electron excitation in producing the emission lines and need to be included in the model calculations before a comprehensive analysis can be attempted.

Subject headings: ISM: individual (SN 1006) — ISM: supernova remnants — shock waves — ultraviolet: ISM

1. INTRODUCTION

SN 1006 is the relatively young remnant of a Type Ia supernova in our Galaxy. At X-ray and radio wavelengths it shows a nearly circular, strongly limb-brightened shell structure (Pye et al. 1981; Reynolds & Gilmore 1986). Proper motion and velocity measurements provide a distance estimate of 2 kpc (Long, Blair, & van den Bergh 1988) and a diameter estimate of 18 pc, implying a mean expansion rate of ~8700 km s^{-1}. The only optical emission is a faint filament of pure Balmer line emission that stretches across the NW sector of the remnant (van den Bergh 1976; Schweizer & Lasker 1978; Long et al. 1988; Winkler & Long 1995). The unusual optical spectrum and the two-component Hα profile imply that the optical emission arises from partially neutral material entering a fast nonradiative shock (Chevalier & Raymond 1978; Chevalier, Kirshner, & Raymond 1980). The ~2300 km s^{-1} width of the broad component of Hα in SN 1006 implies a shock velocity of 2400–3200 km s^{-1}, depending on the level of electron-ion temperature equilibration (Smith et al. 1991). The lower velocity corresponds to very weak electron heating in the shock, and the higher to equal electron and ion temperatures.

Despite its faintness, SN 1006 is an attractive target for UV observations because it is at relatively high Galactic latitude (~14°.6) and has only modest foreground reddening. Schweizer & Middleditch (1980) derive $E(B-V) = 0.112 \pm 0.024$ for a subdwarf OB star now known to lie behind the remnant (see Fesen et al. 1988; Wu et al. 1993). Ultraviolet emission lines from nonradiative shocks arise in a narrow ionization zone just behind the shock front (in contrast to *radiative* shocks, where the emission arises in a cooling zone downstream). Therefore, observations of such shocks can be used to study electron-ion equilibration and perhaps the cosmic-ray acceleration process in collisionless shocks (Raymond et al. 1983; Long et al. 1992; Hester, Raymond, & Blair 1995). However, the UV emission from such shocks is very faint and has previously been detected only in spectra of a few nonradiative positions in the Cygnus Loop. We have detected faint UV emission from SN 1006 using the Hopkins Ultraviolet Telescope (HUT) on the Astro-2 space shuttle mission in 1995 March. As in the Cygnus Loop nonradiative filaments, the SN 1006 spectrum shows only emission from He II, C IV, N V, and O VI in the UV. We believe that a broad Lyβ line from the remnant is also detected underlying the airglow emission. In the following sections we present the line intensities and line widths, followed by a brief discussion of the implications of this unique measurement.

2. OBSERVATIONS AND REDUCTIONS

A technical description of the HUT instrument as flown on the Astro-1 mission is given by Davidsen et al. (1992). New optical coatings on the 0.9 m primary mirror and on the spectrograph grating improved the sensitivity by a factor of 2.3 for Astro-2 (Kruk et al. 1995). Far-ultraviolet spectra covering the 820–1840 Å spectral range at ~3 Å resolution were obtained with HUT during two separate pointings during Astro-2, on 1995 March 12 and 15. HUT has enormous sensitivity to faint, diffuse sources like SN 1006 because of its large spectrograph entrance apertures and f/2 beam. We used the largest aperture available, 19″ × 197″. This slit can only be used during orbital night periods because the strength of the Lyα airglow line could prove to be dangerous to the detector. Use of this slit degrades the spectral resolution to 5–6 Å if its

[1] Astro-2 Guest Investigator.

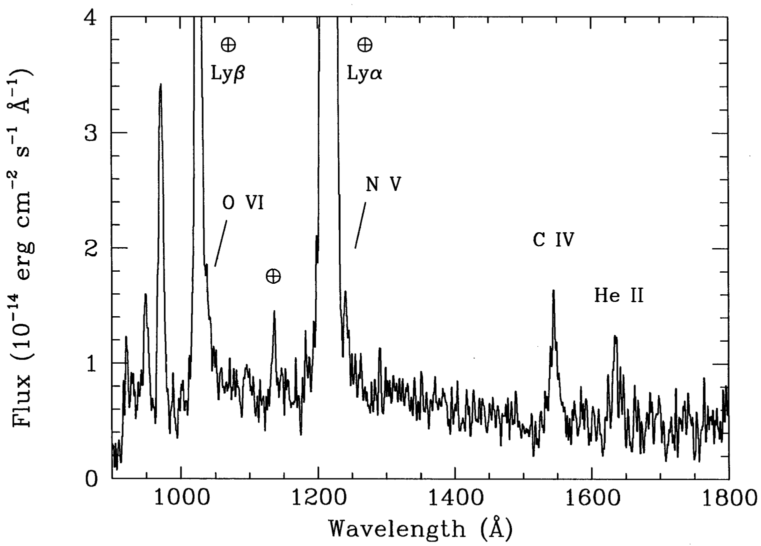

FIG. 2.—Flux-calibrated FUV spectrum of SN 1006 obtained with HUT. Airglow lines are marked with an Earth symbol. (Lyγ and Lyδ are also visible.) A Gaussian smoothing with $\sigma = 1.5$ bins (0.51 Å bin^{-1}) has been applied. Note the broad, asymmetric red wing on Lyβ indicating the presence of O VI.

width is filled with emission. Data from the daytime portion of the first pointing using a smaller (10″ × 56″) slit show weaker signal and are heavily contaminated by airglow. Here we consider only 1478 s of low background orbital night data derived from the two pointings.

The aperture was placed at a position angle of 55°, roughly aligned with a bright portion of the optical filament, as shown in Figure 1 (Plate L2). The position was fixed by acquisition of preplanned guide stars, which were also used for tracking during the integrations. As shown in the figure, we placed the aperture a few arcseconds toward the inside of the Balmer filament, because model calculations indicate the O VI emission should peak 5″–10″ behind Hα. The spectra were reduced using a special HUT package developed within IRAF and the calibration described by Kruk et al. (1995). The uncertainties in wavelength are less than 0.2 Å and those in intensity calibration are less than 5%.

The flux-calibrated spectrum of SN 1006 is shown in Figure 2. The emission features of He II, C IV, N V, and O VI are indicated. The N V doublet can be seen more clearly by comparison against a Lyα airglow template. Likewise, the blended O VI doublet is seen as as asymmetric wing on the red side of the Lyβ airglow line. This spectrum represents the first successful detection of UV emission lines from SN 1006, and only the fourth galactic remnant with detected O VI emission (see Blair, Raymond, & Long 1995).

To extract fluxes, we have used a nonlinear χ^2 minimization routine called SPECFIT within the HUT package in IRAF to fit line profiles and a linear local background to each region of interest (see Kriss 1994). We assumed Gaussian line profiles for O VI, N V, and C IV, and fixed the relative wavelengths and 2:1 relative intensities of the doublets. For O VI, we also constrained the line width to be less than 3100 km s^{-1} (but let the absolute wavelength vary).[2] As discussed below, we expect a broad Lyβ line from SN 1006, so we include that in the fit, with its width constrained to be less than 3100 km s^{-1}. For the Lyβ airglow line, we created a hybrid profile corresponding to a square profile at the aperture width smoothed by a Gaussian at the instrumental resolution. The final fit for the Lyβ-O VI region is shown in Figure 3. A template Lyα profile constructed from airglow observations through the same aperture was used in the fit of the N V region. C IV is the best feature for measuring line widths, since it is relatively strong and uncontaminated by airglow. Figure 4 shows the C IV profile and fit.

Table 1 presents the emission line fluxes, velocities, and velocity widths (FWHM) for the five line features detected, along with the Hα flux within the HUT aperture derived from the CTIO 4 m CCD image of Winkler & Long (1995). We have assumed that their 25 Å wide Hα filter accepted all of the narrow component flux and 1/3 of the broad component, and that the intensity ratio of the two components is as measured by Smith et al. (1991); thus, we multiply the flux obtained from the Winkler and Long calibration by a factor of 1.44. The Hα broad component flux implies (in conjunction with the relative 3*s*, 3*p*, and 3*d* excitation rates of Smith, Laming, & Raymond 1995) a Lyβ broad component of comparable width to the O VI line and about 1.5 times as strong. The interstellar Lyβ absorption will remove the central 1/3 of the line, but this is buried under the airglow feature anyway. The blue wing of Lyβ in Figure 3 clearly corresponds to broad Lyβ from SN 1006. Its intensity is about twice that expected, but the uncertainties in both the measurement and the prediction are substantial. Higher Lyman lines may also be present under the airglow features, and the confluence of Lyman lines may account for the emission just above the Lyman edge. Table 1 also gives the flux of the faint continuum in the 1000–1100 and 1350–1450 Å bands (after subtraction of airglow—see below). The table also includes intensity values corrected for $E(B-V) = 0.11$ using the reddening curve of Longo et al. (1989).

The line centroids are consistent with 600–1000 km s^{-1} blueshifts for C IV and He II and a redshift of comparable magnitude for O VI. This is not expected for a shock viewed essentially edge-on (although a similar shift was reported for the Hα profile of a filament in Tycho's SNR—see Smith et al. 1991). Displacements perpendicular to the dispersion within the HUT large aperture could cause relative shifts by ±3 Å, which is roughly what is observed. This could indicate that C IV

[2] While the assumption that O VI is optically thin can be questioned for slower SNR shock waves (Raymond et al. 1988; Cornett et al. 1992), it is appropriate for the broad lines in SN 1006.

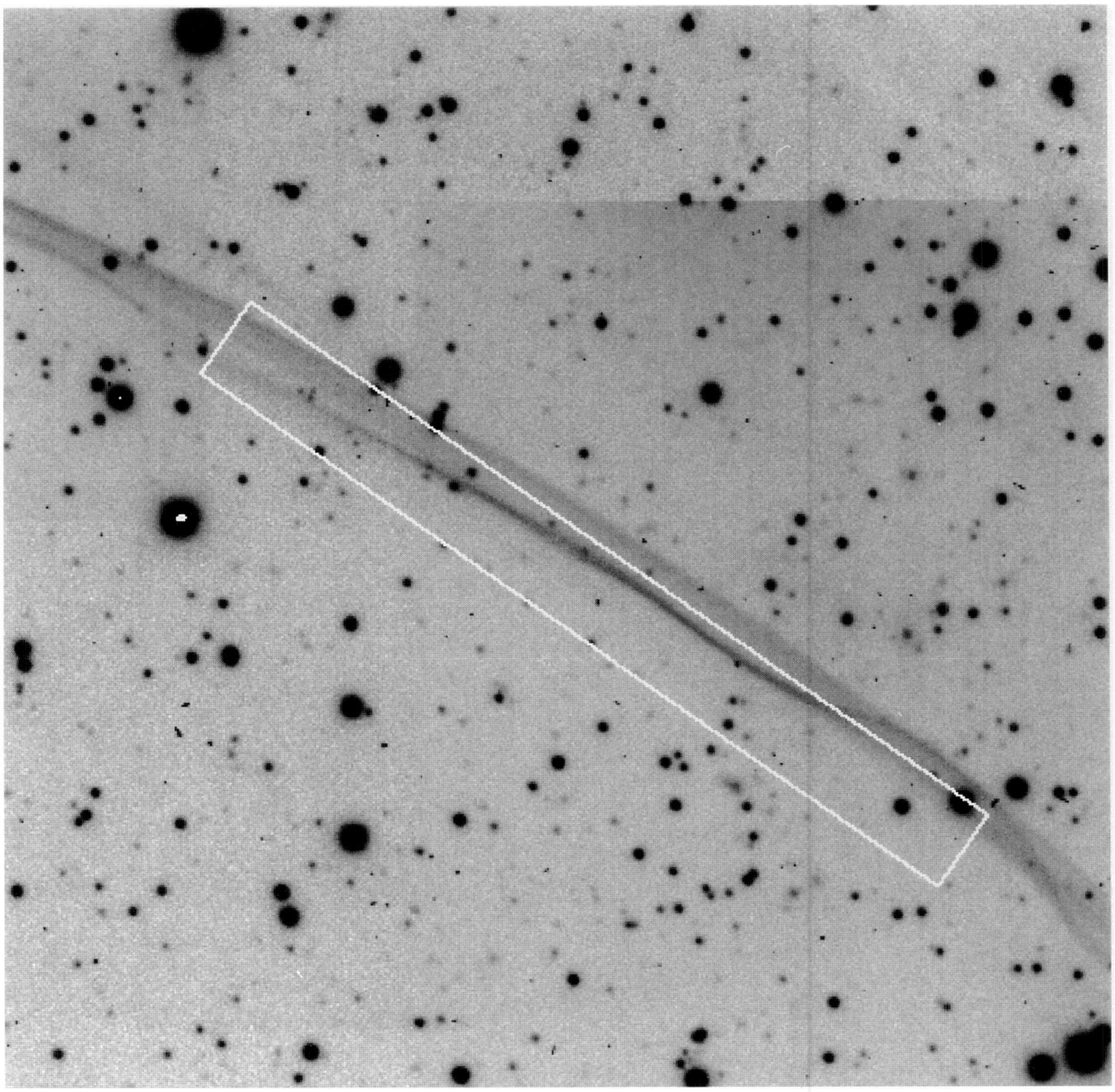

FIG. 1.—Hα CCD image of the NW region of SN 1006, obtained with the CTIO 4 m telescope (Winkler & Long 1995). The position and orientation of the HUT 19″ by 197″ aperture are shown by the box. The sharp edge to the NW of the filament arises from a combination of two images and is not real.

RAYMOND, BLAIR, & LONG (see 454, L32)

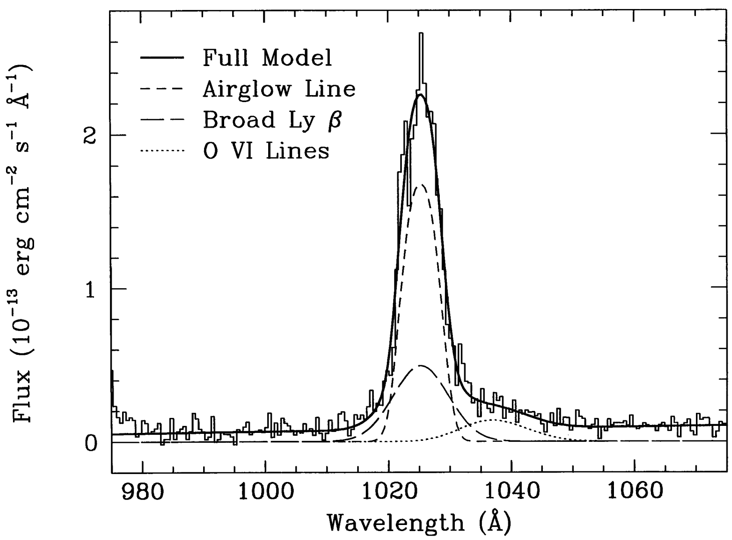

FIG. 3.—Enlargement of the Lyβ O VI region showing the data (*histogram*) and the best fit to the emission feature (*solid heavy line*). See text for details of fit, which includes a Lyβ airglow line and broad Lyβ and O VI from the remnant.

and He II are skewed toward the NW side of the aperture, while O VI is skewed toward the SE, as expected. This also raises the possibility that only a portion of the O VI emission was sampled by the aperture.

The velocity widths presented in Table 1 need to be corrected for the instrumental profile. The spectrum of a much slower shock in the Vela SNR (for which we believe C IV emission fills the slit) shows a C IV FWHM of only 4.6 Å. If we assume that this represents the instrumental width, the intrinsic C IV line width is 2486 ± 379 km s^{-1}. The He II width is comparable, but more uncertain. If the emission from the SNR does not fill the slit, the actual instrumental profiles could be somewhat narrower (and hence the intrinsic widths slightly larger).

A faint continuum is seen in the HUT spectrum after careful subtraction of dark counts and scattered Lyα airglow. Comparison with orbital night airglow spectra shows that it is real. R. Cornett (1995, private communication) reports that UIT detected no UV bright stars within the HUT aperture to a level a factor of 50 below the HUT detection. While the residual continuum is noisy, its shape resembles the spectrum of a B star. It is about 6 times as bright as the typical Galactic dust-scattered stellar background, and about 1/3 as bright as the maximum UV background brightness. A *Voyager* observation of the SN 1006 region shows a continuum level of 8.4×10^{-15} ergs cm^{-2} s^{-1} Å^{-1}, consistent with our value, confirming galactic background as the source (J. Murthy 1995, private communication). Unfortunately, it precludes detection of the hydrogen two-photon continuum seen in the nonradiative shock waves in the Cygnus Loop (Hester et al. 1994).

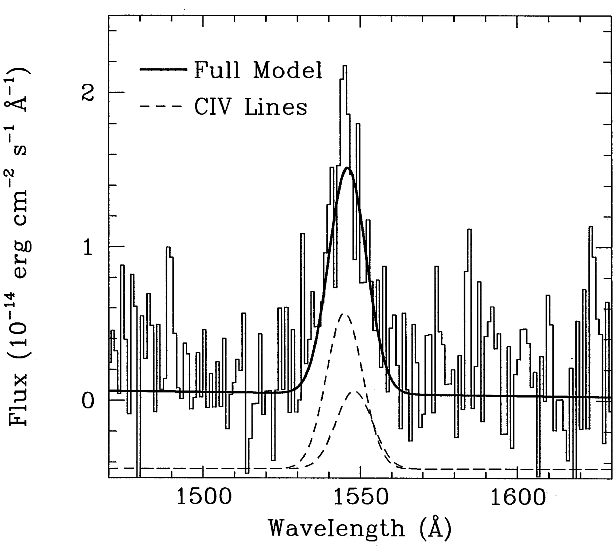

FIG. 4.—Enlargement of the C IV region showing the data (*histogram*) and the best fit to the emission feature (*solid heavy line*), assuming λ1548:λ1551 = 2:1. The individual Gaussian components are shown as dashed lines. Note the obvious blueshift to the line centroid.

3. DISCUSSION

A central question in collisionless shock wave physics is the degree of electron-ion and ion-ion temperature equilibration. If the shock simply randomizes particle velocities, the ions carry nearly all the bulk kinetic energy of the preshock flow, so they will have nearly all the thermal energy behind the shock. A heavier ion carries proportionately more energy. Coulomb collisions will transfer energy among the ions and from ions to electrons, but the rates are relatively slow, and they decrease with increasing temperature. Plasma turbulence within the shock front may transfer energy much more rapidly, but the rate is difficult to determine. The hybrid plasma code of Cargill & Papadopoulos (1988) predicts electron and ion temperatures $T_e \simeq 0.25T_i$ for a Mach 50 shock, but the neutrals which must be present in a Balmer line filament may damp out plasma turbulence. The intensity ratios of the broad and narrow Hα components in nonradiative shocks depend on T_e through the ratio of ionization and charge transfer rates, and the observed ratios provide evidence that electron and ion temperatures do not reach equilibrium, though they may be consistent with the Cargill & Papadopoulos (1988) predictions (Smith 1991; Smith et al. 1995).

The HUT observations lead to one model-independent conclusion: plasma turbulence in the shock front is *not* effective in producing temperature equilibration among the differ-

TABLE 1

MEASURED AND DEREDDENED FLUXES

Ion	F_λ[a]	I_λ[b]	Centroid (km s^{-1})	FWHM (km s^{-1})
Lyβ broad	5.56 ± 0.93	21.0 ± 3.5	−126 ± 23	3100 (fixed)
O VI	1.85 ± 0.26	7.00 ± 0.98	1026 ± 377	3100 (fixed)
N V	1.08 ± 0.19:	2.82 ± 0.50:	...	2800 (fixed)
C IV	1.87 ± 0.20	4.21 ± 0.45	−624 ± 132	2641 ± 355
He II	1.17 ± 0.20	2.4 ± 0.41	−965 ± 254	2558 ± 618
Hα	1.94 ± 0.95[c]	2.33 ± 1.11	...	2230 ± 210[d]
F(1000–1100)[e]	7.30 ± 1.02	26.9 ± 3.8	...	...
F(1350–1450)[e]	5.60 ± 0.70	14.3 ± 1.8	...	...

[a] In units of 10^{-13} erg cm^{-2} s^{-1}; errors are 1 σ.

[b] Reddening corrections assume $E(B-V) = 0.11$ and a standard Galactic extinction curve: see text.

[c] Derived from Hα image of Winkler & Long 1995.

[d] From Smith et al. 1991.

[e] Average continuum fluxes in units of 10^{-15} ergs cm^{-2} s^{-1} Å^{-1} over the indicated range, after subtraction of an airglow spectrum. Errors are 1 σ over 10 Å bins.

ent ion species. If the kinetic temperatures of H, He, C, N, and O were equal, the line widths would scale inversely as the square root of the atomic weight. From the 2230 km s^{-1} Hα width, one would expect He II and C IV widths of 1115 and 644 km s^{-1}, and these are inconsistent with the observations. Considering the large uncertainties of the O VI and N V line widths, we conclude that all the observations are consistent with simple randomization of 3/4 of the shock velocity, and there is no detectable redistribution of energy among the ions within the region sampled by our observations. This strongly suggests that plasma turbulence does not equilibrate electron and ion temperatures, since any waves that interact effectively with the protons would probably interact with He and other ions as well.

The extinction-corrected intensity ratios of Hα, He II, N V, and O VI relative to C IV are 0.51, 0.58, 0.68, and 1.77, respectively. These are consistent to within a factor of 2 with model predictions for a 2300 km s^{-1} shock in cosmic abundance gas which is 50% neutral ahead of the shock. The model was computed with the code used by Hartigan, Raymond, & Hartmann (1987), the assumption of pure Coulomb ion-ion and electron-ion equilibration, and a column density cutoff to avoid the postshock cooling region. Thus, the UV and Hα line strengths and widths appear to be consistent with non-equilibrated electron and ion temperatures. However, the model does not yet include proton excitation, and detailed interpretation would be premature. Based on the semiclassical approximations of Walling & Weisheit (1988), we believe that excitation by protons exceeds the electron excitation rates for the O VI, N V, and C IV lines. In weakly equilibrated models, much of the UV line emission occurs at a few million K, while Cargill & Papadopoulos (1988) predict $T_e \simeq 2 \times 10^7$ K at the shock. We hope that when the model calculations are complete, we will be able to discriminate between these predictions.

We thank our many colleagues on the HUT team and all of the NASA personnel who helped to make Astro-2 happen. We also thank Frank Winkler for providing access to his Hα image prior to publication, and Jayant Murthy for consultation about *Voyager* UV background levels. Support for this work is provided by NASA Grant NAG8-1074 to the Smithsonian Astrophysical Observatory and NASA contract NAS5-27000 to the Johns Hopkins University.

REFERENCES

Blair, W. P., Raymond, J. C., Long, K. S., & Kriss, G. A. 1995, ApJ, 454, L35
Cargill, P. J., & Papadopoulos, K. 1988, ApJ, 329, L29
Chevalier, R. A., Kirshner, R. P., & Raymond, J. C. 1980, ApJ, 235, 186
Chevalier, R. A., & Raymond, J. C. 1978, ApJ, 225, L27
Cornett, R. H., et al. 1992, ApJ, 395, L9
Davidsen, A. F., et al. 1992, ApJ, 392, 264
Fesen, R. A., Wu, C. C., Leventhal, M., & Hamilton, A. J. S. 1988, ApJ, 327, 178
Hamilton, A. J. S., & Fesen, R. A. 1988, ApJ, 327, 178
Hartigan, P., Raymond, J. C., & Hartmann, L. 1987, ApJ, 316, 323
Hester, J. J., Raymond, J. C., & Blair, W. P. 1994, ApJ, 420, 721
Kriss, G. A. 1994, in ASP Conf. Ser. G1, Astronomical Data Analysis Software & Systems III, ed. D. R. Crabtree, R. J. Hanisch, & J. Barnes (San Francisco: ASP), 437
Kruk, J. W., Durrance, S. T., Kriss, G. A. Davidson, A. F., Blair, W. P., Espey, B. R., & Finley, D. S. 1995, ApJ, 454, L1
Long, K. S., Blair, W. P., Vancura, O., Bowers, C. W., Davidsen, A. F., & Raymond, J. C. 1992, ApJ, 400, 214
Long, K. S., Blair, W. P., & van den Bergh, S. 1988, ApJ, 333, 749
Longo, R., Stalio, R., Polidan, R. S., & Rossi, L. 1989, ApJ, 333, 749
Pye, J. P., Pounds, K. A., Rolf, D. P., Smith, A., Willingale, R., & Seward, F. D., 1981, MNRAS, 194, 569
Raymond, J. C., Blair, W. P., Fesen, R. A., & Gull, T. R. 1983, ApJ, 275, 636
Raymond, J. C., Hester, J. J., Cox, D. P., Blair, W. P., Fesen, R. A., & Gull, T. R. 1988, ApJ, 324, 869
Reynolds, S. P., & Gilmore, D. M. 1986, AJ, 92, 1138
Schweizer, F., & Lasker, B. M. 1978, ApJ, 226, 167
Schweizer, F., & Middleditch, J. 1980, ApJ, 241, 1039
Smith, R. C. 1991, Ph.D. thesis, Harvard Univ.
Smith, R. C., Kirshner, R. P., Blair, W. P., & Winkler, P. F. 1991, ApJ, 375, 652
Smith, R. C., Laming, J. M., & Raymond, J. C. 1995, in preparation
van den Bergh, S. 1976, ApJ, 208, L17
Walling, R. S., & Weisheit, J. C. 1988, Phys. Rep., 162, 1
Winkler, P. F., & Long, K. S. 1995, in preparation
Wu, C. C., Crenshaw, D. M., Fesen, R. A., Hamilton, A. J. S., & Sarazin, C. L. 1993, ApJ, 416, 247